

© 2020. W. Hernandez, A. Viviescas, C.A. Riveros-Jerez.

This is an open-access article distributed under the terms of the Creative Commons Attribution-NonCommercial-NoDerivatives License (CC BY-NC-ND 4.0, <https://creativecommons.org/licenses/by-nc-nd/4.0/>), which permits use, distribution, and reproduction in any medium, provided that the Article is properly cited, the use is non-commercial, and no modifications or adaptations are made.



# VERIFYING OF THE FINITE ELEMENT MODEL OF THE BRIDGE BASED ON THE VIBRATION MONITORING AT DIFFERENTE STAGES OF CONSTRUCTION

W. HERNANDEZ<sup>1</sup>, A. VIVIESCAS<sup>2</sup>, C.A. RIVEROS-JEREZ<sup>3</sup>

This paper presents the results of a dynamic response evaluation of a segmental bridge during two construction stages: before connecting the final segment of the bridge and after connecting the final segment of the bridge but prior to opening the bridge to traffic. The vibration signals obtained from Ambient Vibration Testing (AVT) campaigns were processed in order to obtain the modal parameters of the bridge during the two construction stages. Modal parameters experimentally obtained for the first stage were compared with those obtained from Finite Element (FE) models considering different construction loads scenarios. Finally, modal parameters experimentally obtained for the second stage were used to update its corresponding FE model considering two scenarios, before and after the installation of the asphalt pavement. The results presented in this paper demonstrated that a rigorous construction control is needed in order to effectively calibrate FE models during the construction process of segmental bridges.

*Keywords:* segmental bridge, modal identification, FE model updating, ambient vibration testing.

<sup>1</sup> M.Eng (c), Eng., Industrial University of Santander, School of Civil Engineering, Bucaramanga, Colombia, e-mail: wilson.hernandez@correo.uis.edu.co

<sup>2</sup> Assoc. Prof., PhD., Eng., Industrial University of Santander, School of Civil Engineering, Bucaramanga, Colombia, e-mail: alvivija@uis.edu.co

<sup>3</sup> Assoc. Prof., Dr. Eng., Eng., University of Antioquia, Faculty of Engineering, Medellin, Colombia, e-mail: carlos.riveros@udea.edu.co

## 1. INTRODUCTION

Structural monitoring of bridges is becoming increasingly important as advanced monitoring systems are developed and their associated costs are gradually reduced. A great potential to predict abnormal structural behaviour in its early stage has motivated the research community and government agencies to conduct experimental campaigns using Ambient Vibration Testing (AVT) [1-5]. Although there still remain several environmental issues to be fully understood in order to accurately monitor the response of a bridge under continuous operation, the structural monitoring technology developed during recent years allow those experimental campaigns to be conducted for fully operational bridges with easy-to-deploy and install equipment as reported by [1,6,7]. Structural monitoring is then a useful tool in seismically active areas to assess structural integrity after a seismic event, environmental degradation or extreme loading condition, which are the most common causes of bridge failures in Colombia. AVT is based on the analysis of structural response under the action of ambient excitation sources such as wind, traffic, seismic events, or wave loading. The main assumption when considering AVT is that ambient excitation nearly always is broad-banded [8]. Although several AVT campaigns have been conducted for fully operational bridges by several studies [6,9-12], limited information regarding AVT campaigns during construction of bridges is reported in the literature. Colombia is recently experiencing a rapid economic growth leading to high public investment in infrastructure. Major Colombian urban centers are therefore demanding efficient and rapid regional infrastructure connectivity. It is then important to highlight that bridge construction in Colombia requires the development and implementation of local control construction procedures in order to guarantee safe and durable structures. Moreover, it is important to develop such procedures to early detect any abnormal response of a bridge during its construction process. Bucaramanga is the fifth largest Colombian city located on a plateau and separated from the municipality of Floridablanca by a Canyon. The existing road infrastructure between Bucaramanga and Floridablanca mainly relied on the Garcia Cadena viaduct, which became insufficient to existing traffic demand and therefore it was necessary the construction of a new parallel viaduct called La Unión viaduct. AVT campaigns were conducted during the construction stage of La Unión viaduct in order to characterize the inherent variation of its dynamic response, since it is the most vulnerable stage of the structure to collapse. The objective of the AVT campaigns was the calibration of the previously assembled FE model in order to compare the dynamic response of the bridge to the one obtained when the construction of the bridge

was finished but prior to traffic opening. In addition, possible drawbacks and limitations in application of AVT to update FE models during the construction stage of the bridge are also addressed.

## 2. BRIDGE DETAILS

As previously mentioned, the primary objective of the new bridge project was to ease traffic congestion on the existing Garcia Cadena viaduct connecting Bucaramanga and Floridablanca. The newly constructed viaduct (La Unión) runs parallel to the existing viaduct (Garcia Cadena) and has a total length of 278 m considering the post-tensioned concrete beams in the north access (Bucaramanga side), the 2 ribbed slabs in south access (Floridablanca side) and a three-span bridge structure. The length of bridge structure including main span and side spans is 218.95 m with a constant width of 22.5 m. The three-span bridge structure consists of segments with variable section height placed in a successive cantilever fashion. The length of main span is 110 m with two side spans of 52.45 m and 55.5 m as shown in Fig 1 (a). The bridge superstructure consists of a tricellular concrete box girder of varying height: 2.5 m to 6 m as shown in Fig 1 (b). 2 pairs of hollow-section pylons/towers 22 m height are located at each end of the main span. The pylons are supported on rectangular pile caps (20 m length and 11 m wide) with 1.5 m diameter piles. The length of the piles varies from 20 m to 25 m. The dynamic response assessment during the construction of the bridge is divided into two phases. The first phase corresponds to the construction stage before connecting the final segment of the bridge, and before connecting the bridge to the access segments in each side of the bridge. The north section consists of 13 pairs of segments with a total length of 100 m and the south section consists of 14 pairs of segments with a total length of 108.50 m. During this stage it is considered the loading effect of the formwork traveller and the construction materials placed on the superstructure of the bridge. It is not expected large fluctuations in dead weight and live load along the span length during field testing and therefore such associated load variations are not considered. The AVT campaigns were carried out without interrupting the construction of the bridge and according to the construction instructions provided by the bridge contractor (Consorcio Vial Puerta de Sol). The second stage is defined before connecting the final segment of the bridge but prior to opening the bridge to traffic. During this stage 3 AVT campaigns were carried out before and after the installation of the asphalt pavement in order to study the influence of the asphalt pavement in the dynamic response of the bridge.

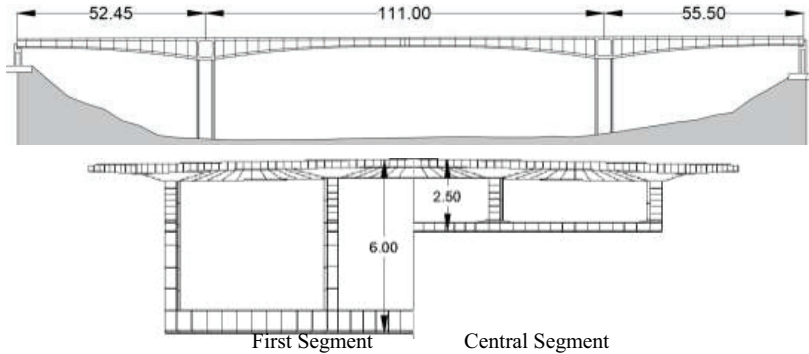


Figure 1. a) La Unión viaduct side view, b) La Unión viaduct cross section. Source: The authors.

### 3. FE MODELLING

#### 3.1. GENERAL CONSIDERATIONS

The FE models of the bridge during the different construction stages presented in this paper are assembled in MIDAS engineering software [13]. The geometry, material properties, and load considerations used in the FE models are based on the construction drawings supplied by the bridge contractor. Considering that the response of the bridge under ambient excitation loads such as traffic or wind leads to a linear structural response, material nonlinearity is not considered and therefore modal analysis is performed. In addition, creep, shrinkage, temperature and time-dependent effects are not considered in the FE Models. According to the information provided in the as-built drawings, the Young's modulus ( $E_c$ ) is numerically determined in accordance with the recommendation of the Colombian bridge code CCP-14 (5.4.2.4) [14] using the following formula.

$$(3.1) \quad E_c = 4800\sqrt{f'_c}.$$

Where  $f'_c$  - specified compressive strength of concrete ( $f'_c$ ) defined by the pylons is 28 MPa and 35 MPa is defined for the segmental beams.

As previously mentioned, ambient excitation loading such as traffic or wind cannot generate sufficient force to excite the bridge within a non-linear regime. As a result, a linear response of the bridge is assumed by considering as well that in a newly constructed structure time-dependent material properties or load-time dependent effects do not affect its dynamic response. Kerr [15]

experimentally demonstrated that the dynamic response of a prestressed beam is not affected by the cable tension force for a cable located in its cross section. On the other hand, Materazzi et al. [16] and Breccolotti et al. [17] concluded that the prestress effects cannot be ignored under non-linear structural response. The prestress force action modifies the stiffness matrix and the Young's modulus thus affecting the dynamic properties. Therefore, the FE models presented in this paper do not consider the prestress force effects. A solid element type is used to assemble the FE model. To validate the density of the finite element mesh it is performed a sensitivity analysis using 6 models in each of the presented segments by considering 1000, 5000, 10000, 15000, 25000, 35000, 45000 elements. The sensitivity analysis objective is to evaluate the incidence of the finite element mesh in the dynamic properties. The numerically obtained mode shapes contributing significantly to the mass of the bridge in each direction are used to plot the variation of the period as a function of the number of FE elements. The FE model is defined within a global coordinate system where the longitudinal direction corresponds to the  $x$ -axis, the transversal direction to the  $y$ -axis and the vertical direction to the  $z$ -axis.

### 3.2. CONSTRUCTION STAGE 1

A vertical double-column pylon is the support system for each of the segments presented in the construction stage 1. Fixed supports are considered to assemble the FE model for the construction stage 1. AVT campaigns were conducted before the construction of the connecting segment between the north and the south sections considered in the construction stage 1, therefore, boundary conditions are not considered acting on the final segments of each of the FE models assembled in the construction stage 1. The types of permanent loads employed in the FE models are: self-weight (DC), formwork traveller weight (FT), and live load during construction (CLL). An imposed load value of  $19.61 \text{ kN/m}^2$  adopted in AASTHO LRFD Bridge Design Specification [18] is selected based on a thorough study conducted by the authors considering different design guidelines, technical recommendations, and bridge codes. The weight of the formwork traveller adopted in the FE models corresponds to 1067.57 kN according to the design specification provided by the bridge contractor. The load due to weight of the formwork traveller and the segment under construction are assigned to the FE models as concentrated loads and placed on the section segments where anchorage is generated. It is assumed that wind loads acting on the superstructure as well as on construction machinery are the main excitation sources during field testing. The sensitivity analysis performed is based on the aforementioned approach showed that the variation of the evaluated parameter is asymptotic as shown in Fig. 2 (a) (b). The selected finite element mesh for the FE

models in this construction stage corresponds to 3500 elements. The FE model of the north section considering support conditions, imposed load cases and the material types used in the bridge segments and pylons are shown in Fig. 2 (c). The dynamic parameters resulting from the FE models assembled in MIDAS engineering software [13] were obtained using the Lanczos method. Tridiagonal Matrix is then used to perform eigenvalue analysis. Fig. 3 shows the numerical results of the three mode shapes with the large modal mass participation factor considering each of the orthogonal directions.

### 3.3. CONSTRUCTION STAGE 2

As previously mentioned, once the final segment of the bridge is constructed and prior to opening the structure to traffic, the modal response of the bridge is obtained prior to the installation of the asphalt pavement. Then, after installing the asphalt pavement modal response of the bridge is newly obtained. Therefore, the asphalt pavement load is the only factor that differentiates the two FE models presented in this paper for the construction stage 2. Thickness of asphalt pavement layer is 100 mm. The load values used in the FE models for the different components are  $0.5 \text{ kN/m}^2$  for the steel guardrail,  $12 \text{ kN/m}^2$  for the concrete barrier,  $4.4 \text{ kN/m}^2$  for the sidewalk, and  $2.2 \text{ kN/m}^2$  for the asphalt pavement. Fig. 4 shows the numerically obtained mode shapes with the large modal mass participation percentage considering each of the orthogonal directions for the FE model with asphalt pavement.

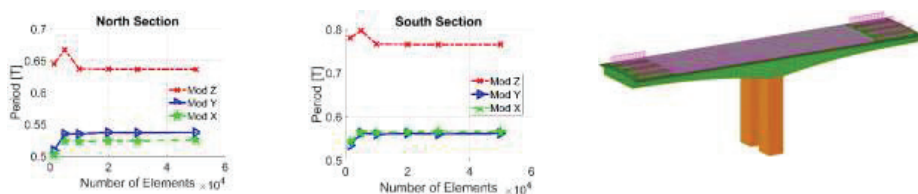


Figure 2. a) Calibration period vs number of elements (north section), b) Calibration period vs number of elements (south section), c) Imposed Loads, Bridge Segments and Pylon (FE Model North Section). Source: The authors.

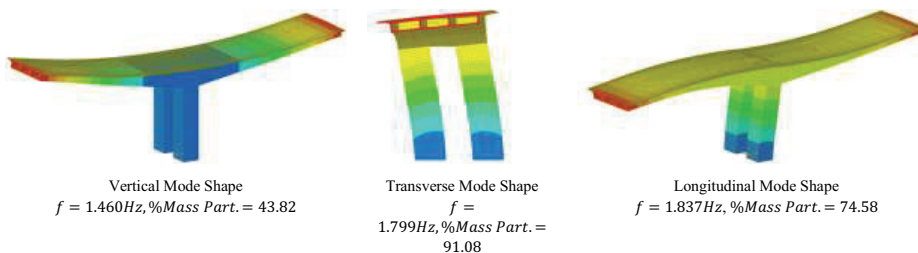


Figure 3. Numerical Mode Shapes (North Section). Source: The authors.

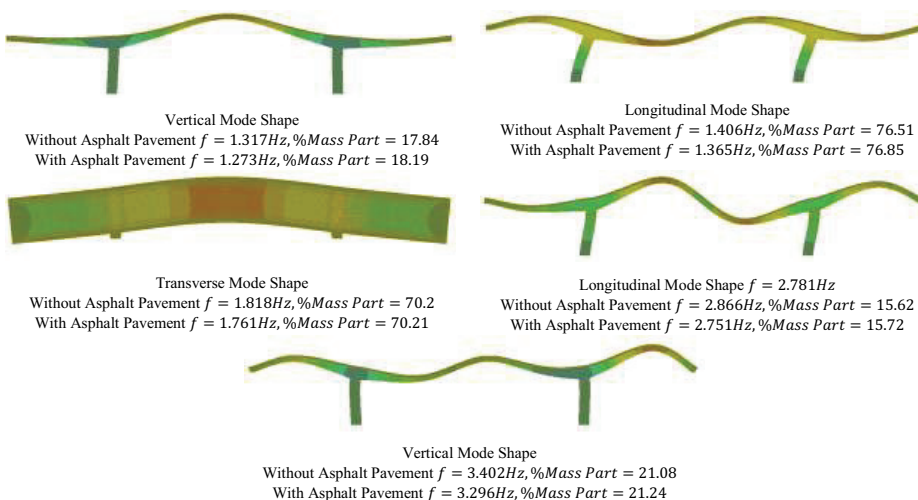


Figure 4. Numerical Mode Shapes (Construction Stage 2). Source: The authors.

## 4. AVT CAMPAIGNS

### 4.1. GENERAL CONSIDERATIONS

In the present study, the main external factors assumed to cause vibrations are wind load on the superstructure and construction machinery excited mainly by wind, less important external factors are microseisms and anthropic loads. 3 high sensitivity accelerometers Obsidian Kinematics® [19] were deployed in order to acquire and process data from the vibration signals using GPS synchronization. Then, a sampling rate of 1200 samples/second is selected in order to adequately satisfy the Nyquist sampling criteria [20]. A 1024 point FFT, and 66% overlapping Hanning

window are applied to the input data. The EFDD method included in the software ARTeMIS [21] is used to obtain modal frequencies, mode shapes and damping ratios from vibration data. Frequency domain methodologies are based on Peak-Picking (PP) analysis which extracts large energy content peaks which contains information related to modal frequencies. Based on previous studies conducted by [5,22,23], the EFDD method is selected, this method corresponds to an improved version of the FDD method [1] by converting the spectral response matrix into a group of Single-Degree-of-Freedom (SDOF) systems [24,25]. The modal damping ratios are obtained by applying the inverse Fourier transform to the SDOF systems and then evaluating the autocorrelation function decay rate based on the logarithmic decrement approach. The EFDD method based on the aforementioned approach is able to identify modal frequencies close to each other where each modal frequency corresponds to a spectral density functions of a corresponding SDOF system containing information related to modal frequencies, mode shapes and damping ratios [21,26]. Finally, the Modal Assurance Criterion (MAC) index based on generating a reference vector from a correlation analysis index is used to validate the identified mode shapes as recommended [1,27]. Numerical mode shapes obtained from the FE models and experimental mode shapes obtained from vibration data analysis are also analyzed using their corresponding MAC indices. The approach proposed in this paper using multiple measurements obtained from different sensor configurations greatly increases the quality of the identified modal parameters.

## 4.2. CONSTRUCTION STAGE 1

The inherent variability of mass and stiffness of a structure presented during its construction possesses a challenge when sensor placement is conducted. While most studies focus on determining the optimal placement of sensors in operational stage, there are limited studies related to sensor placement during different construction stages. The methodology adopted in this paper is based on recommendations provided by [5,7,11]. Pachón et al. [5] conducted modal identification of the E. Torroja's bridge located in Spain and concluded that using only 4 sensors to perform modal identification, the determined resonant frequencies can be determined with error values less than 2% in comparison to large sensor deployment of 36 measurement points. Therefore, in the present study mode shapes calculated from the FE models are then used to find locations for 3 triaxial accelerometers prior to conduct AVT campaigns. Selected locations in the longitudinal direction are then defined next to the formwork traveller in the extreme end of the cantilever section of the superstructure, the center of the cantilever section of the superstructure and the center of intersection between the double-column pylon and the superstructure. Sensor locations in the



transverse direction are defined at the external ends of the superstructure in order to avoid local vibration response. A total number of 10 selected sensor locations are divided into 2 symmetrically distributed locations of 5 sensors on each side of the superstructure. Fig. 5 shows the identified mode shapes and the identified damping ratios. It is possible to observe that 3 values are lower than the expected range for bridge structures as reported by Chen et al. [1] with values of damping ratios ranging from 0.7% to 3.2%. It is important to note that Tian et al. [28] using impacting test data conducted modal identification of a three-span concrete box girder bridge having similar structural configuration to La Unión viaduct. Multiple reference impact test (MRIT) was used by considering magnitudes of both structural responses and input forces. In addition to 25 accelerometers installed on the bridge, 58 long gauge Fiber Bragg Grating (LG-FBG) strain sensors were also installed. The first 5 vertical natural frequencies and corresponding mode shapes were identified. As previously mentioned, in order to compare the experimentally obtained modal frequencies and mode shapes MAC index is used by comparing obtained modal frequencies from EFDD analysis. Then, MAC index comparison was performed between experimental and numerical modal frequencies showing good correlation. Fig. 6 and 7 show experimental and numerical obtained mode shapes considering both north and south sections. Significant deviations are observed especially in longitudinal and transverse mode shapes. The main source of error may be associated to the concentrated load assumption considered in the FE models. Although concentrated loads were calculated based on the data provided by the bridge contractor and MAC indices show good correlation, load deviations in both magnitude and location of loads may be present during the construction process. It is important to note that construction of the bridge continued during the execution of the AVT campaigns and data related to construction loads were not measured on site. It implies a serious limitation when modal identification is intended to be used to assess structural integrity of a bridge during its construction process.

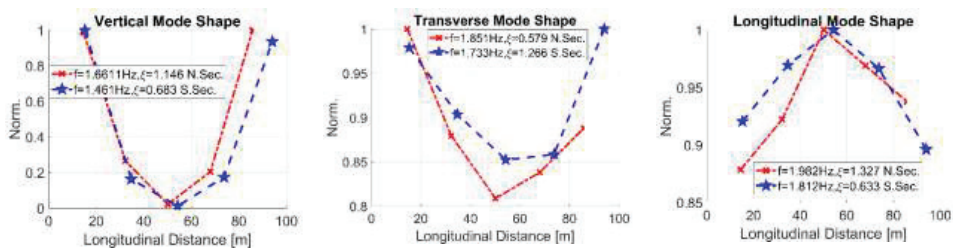


Figure 5. Experimentally Determined Mode Shapes. Source: The authors.

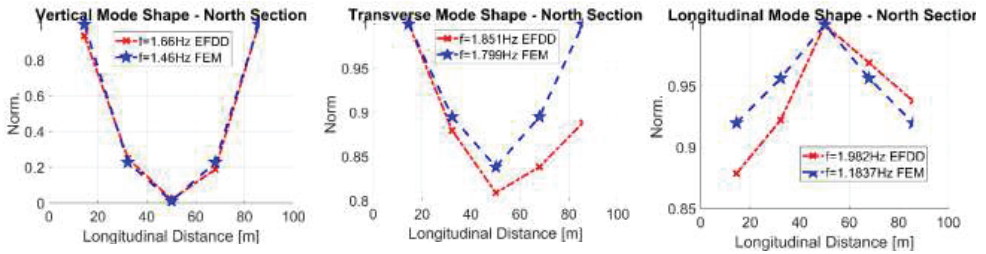


Figure 6. Experimental and Numerical Mode Shapes (North Section). Source: The authors.

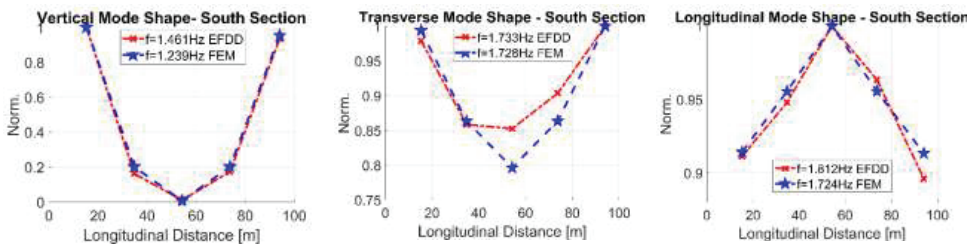


Figure 7. Experimental and Numerical Mode Shapes (South Section). Source: The authors.

### 4.3. CONSTRUCTION STAGE 2

Following the aforementioned sensor placement procedure employed in the construction stage 1, sensor locations in this stage are also selected based on the FE models developed for this construction stage. The first AVT campaign considered a total of 15-minute vibration data collection by locating the reference sensor at one-fifth main span length, the remaining 2 movable sensors were then located at one-fourth cantilever length and one-sixth main span length, respectively. On the cross section, the sensors were located on the outer partitions. The following 2 AVT campaigns considered a total of 20-minute vibration data collection using the same sensor locations along the bridge. Considering the superstructure cross section, sensors are placed in the internal partitions. Fig. 8 shows the experimentally derived mode shapes and corresponding frequencies and damping ratios. The values of damping ratios presented in Fig. 8 are located in the range provided by [1]. Good MAC correlation is also obtained for the 5 identified mode shapes. In addition, it is also observed that the fundamental longitudinal and transverse mode shapes correspond to the fundamental frequencies  $f=1.768$  Hz and  $f=1.821$  Hz, respectively. Fig. 9 shows the comparison between numerical and experimental mode shapes considering the application of asphalt pavement load. Load uncertainty related to concentrated loads in the construction stage 1 is

not relevant in the construction stage 2 because construction of the bridge is already finished thus leading to a more accurate prediction of the mode shapes for the construction stage 2. Experimental modal frequencies considering the application of the asphalt pavement load show modal frequency increment when compared to the ones obtained from the FE model. It can be clearly noticed a tendency of the asphalt pavement to increase bridge rigidity. The results presented in this section are similar to those reported by [1]. They concluded that a sensible insight into the dynamics of a stiff bridge can be achieved by using weak ambient excitation sources. In addition, recent research findings [29] have demonstrated that modal strain energy show less sensitivity to noise in measurement and can be easily derived from the results presented in this section.

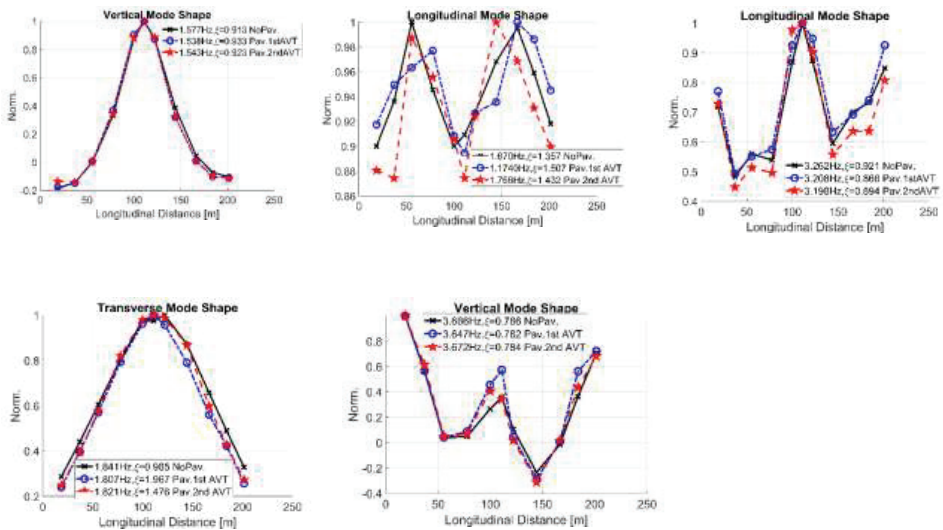
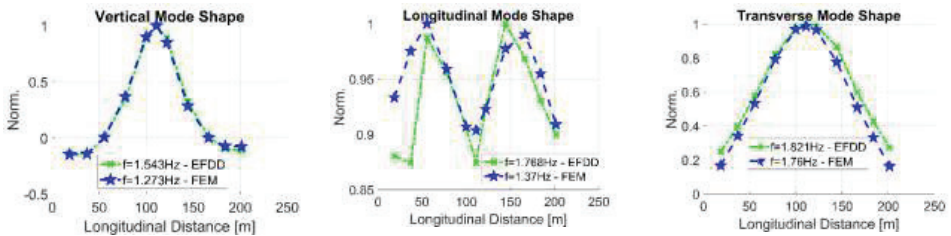


Figure 8. Experimentally Derived Mode Shapes (Construction Stage 2). Source: The authors.



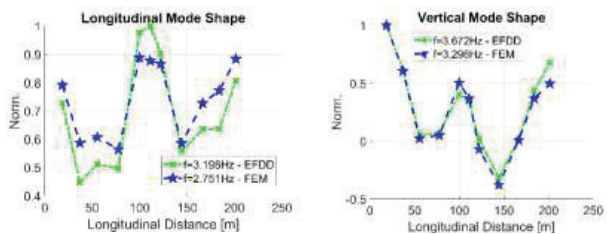


Figure 9. Experimental and Numerical Obtained Mode Shapes (Construction Stage 2). Source: The authors.

## 5. FE MODEL UPDATING

### 5.1. CONSTRUCTION STAGE 1

As previously mentioned, concentrated loads at the extreme ends of the 2 bridges sections in the FE models might be not well approximated by considering the load value of the formwork traveller provided by the bridge contractor. In addition, bridge was under construction when ATV campaigns were conducted possibly leading to the large variations in the identified mode shapes previously reported. Although, it is expected deviations of the Young's modulus and bridge cross sections from the values assumed in the design process, concentrated load assumptions are clearly the most influential factor that cause the significant differences between numerical and experimental derived mode shapes. Accurate calibration of numerical models can be achieved as reported by [2], but it is necessary the combination of field testing with numerical modeling. In the present study, uncertainty mainly arises from the assumed load of the formwork travellers and the segment of the bridge under construction when AVT campaigns were conducted. Considering the formwork traveller load value of 1067.57 kN, which is provided by the bridge contractor, three different load case scenarios are selected in order to study its effect on determining the mass of the superstructure. The superstructure is then analyzed considering variations of load values between the two extreme ends. The extreme end of the superstructure having the lowest load is selected to define the three load case scenarios by selecting load values of 711.72 kN, 889.64 kN and 1067.57 kN. Then, the load values considered in the opposite end of the superstructure varied with increments of 177.93 kN up to 3558.58 kN. A total number of 24 iterations are considered for each of the sections of the bridge studied in the construction stage 1. The percent error is then defined as a function of load variation. It was found that the percent error does not increase as the structural mass is increased

due to extreme ends load variations. Percent error results indicate unbalanced extreme ends loads in north and south sections have values of 711.72 kN and 355.86 kN, respectively. Two variables must be considered when AVT are conducted on a bridge during construction: mass variation due to inherent variability of construction loads (formwork traveller, the segment of the bridge under construction, construction materials, people, construction machinery among others) and stiffness variation caused by material properties due to assumptions during the design process that are considered true and not tested on site. Finally, it is important to emphasize that the analysis presented for the construction stage 1 gives an insight into instrumentation of bridges during different construction stages. Practical applications must incorporate the use of additional instrumentation such strain gauges as reported by [27].

## 5.2. CONSTRUCTION STAGE 2

The main difference between the two construction stages presented in this paper is that construction loads are difficult to measure in practice and therefore there is an additional uncertainty related to structural mass when performing FE analysis. Model updating is then performed for the construction stage 2 based on adjusting the value of the Young's modulus assumed during the design process. The model updating criteria corresponds to adjusting the modal frequency associated to the transverse mode shape taking into consideration the asphalt pavement load. It is also important to note that the experimental results show a more rigid behavior than the numerical modeling. In the construction stage 2 it is treated the Young's modulus as a variable to be updated. The model updating process is carried out by varying the Young's modulus of the double-column pylons while keeping constant the Young's modulus of the superstructure, then keeping constant the Young's modulus of the double-column pylons while varying the Young's modulus of the superstructure. Finally, select the value that most closely approximates the result of the AVT campaigns. The best model is achieved by using  $E_c=49\text{MPa}$  for the double-column pylons and  $E_c=28\text{MPa}$  for the superstructure leading to no increment in the value of the experimental modal frequency while reducing the percent error. Finally, it is also important to highlight that temperature variations and traffic loads definitely produce fluctuations of the estimated natural frequencies as reported by [30].

## 6. CONCLUSIONS

In this paper, a newly constructed triple cell box girder bridge was used to conduct AVT campaigns in order to update previously developed FE models. The main feature which differentiates the results presented in this paper is that the dynamic response of the bridge was carried out for two different construction stages of the bridge. The first construction stage is defined before connecting the final segment of the bridge leading to 2 cantilever-type structures. Significant differences were found between experimental and numerical modeling. Although a parametric study was conducted to study the effect of the construction loads in structural mass, practical limitations related to measure the construction load still remain to be addressed. In addition, construction of the bridge was not suspended during AVT campaigns. Considering that most of the optimal sensor placement methodologies are based on mode shapes information, further research is needed to study the effect of construction loads on experimentally derived mode shapes. The second construction stage is defined after connecting the final segment of the bridge but prior to opening the bridge to traffic. The bridge was then first analyzed before construction of the asphalt pavement to study the influence of the load induced by the asphalt pavement. Most of the studies found in the literature measure dynamic response of bridges in operation thus the influence of this factor in the experimental determination of the bridge response cannot be addressed. Good agreement was found between experimental and numerical modeling for the AVT campaigns conducted before construction of the asphalt pavement. Finally, dynamic response of the bridge was obtained to study the effect of the asphalt pavement load showing good agreement between experimental and numerical modeling. Model updating was then conducted using the FE model loaded with asphalt pavement which corresponds to the monitoring baseline of the bridge that can be used in future to deploy continuous monitoring systems or to study structural degradation of the bridge due to extreme load events. Current bridge design procedures are based on international code standards, design assumptions deviations caused during the construction process need to be verified using field testing data. The approach proposed in this paper uses both numerical and experimental data in order to validate bridge response at different construction stages providing early detection of deviations from bridge design assumptions during construction. Finally, bridge health monitoring cost can be reduced if bridge response is measured during construction.

## REFERENCES

1. G. Chen, P. Omenzetter, S. Beskhyroun, "Operational modal analysis of an eleven-span concrete bridge subjected to weak ambient excitations", *Engineering Structures* 151: 839-860, 2017.
2. C. Costa, D. Ribeiro, P. Jorge, R. Silva, A. Arêde, R. Calçada, "Calibration of the numerical model of a stone masonry railway bridge based on experimentally identified modal parameters", *Engineering Structures* 123: 354-371, 2016.
3. A. Cunha, E. Caetano, F. Magalhaes, C. Moutinho, "From input-output to output-only modal identification of civil engineering structures", In 1st international Operational Modal Analysis Conference, Rune Brincker (Ed.), Copenhagen, Denmark, 2005.
4. X. Min, L. Oliveira, "Dynamic assessment of the São João bridge structural integrity". *Procedia Structural Integrity*, 5: 325-331, 2017.
5. P. Pachón, R. Castro, E. Macías, V. Compan, E. Puertas, "E. Torroja's bridge: tailored experimental setup for SHM of a historical bridge with a reduced number of sensors", *Engineering Structures* 162: 11-21, 2018.
6. A. De-Castro, L. Sánchez-Aparicio, J. Sena-Cruz, D. González-Aguilera, "Integrating geomatic approaches, operational modal analysis, advanced numerical and updating methods to evaluate the current safety conditions of the historical Bóco bridge", *Construction and Building Materials* 158: 961-984, 2018.
7. G. Chio, E. Maldonado, I. Araujo, "Pruebas de vibración ambiental en puentes". *UIS Ingenierías* 9: 55-68, 2010.
8. R. Brincker, L. Zhang, P. Andersen, "Modal identification from ambient responses using frequency domain decomposition", In IMAC 18: Proceedings of the International Modal Analysis Conference (IMAC): A. Moonis (Ed.), San Antonio, Texas, 2001.
9. C. Gentile, N. Gallino, "Ambient vibration testing and structural evaluation of an historic suspension footbridge", *Advances in Engineering Software* 39: 356-366, 2008.
10. F. Magalhaes; E. Caetano, A. Cunha, O. Flamaud, G. Grillaud, "Ambient and free vibration tests of the Millau viaduct: evaluation of alternative processing strategies", *Engineering Structures* 45: 372-384, 2012.
11. W. Ren, W. Zatar, I. Harik, "Ambient vibration based seismic evaluation of a continuous girder bridge", *Engineering Structures* 26: 631-640, 2004.
12. A. Shama, J. Mander, S. Chen, "Ambient vibration and seismic evaluation of a cantilever truss bridge", *Engineering Structures* 23: 1281-1292, 2001.
13. MIDAS Information Technology Co. Ltd. *Midas User Manual*, Seongnam, South Korea, 2016.
14. Instituto Nacional de Vías (INVIAS). *Código Colombiano de Puentes, CCP-14*. Asociación Colombiana de Ingeniería Sísmica: Bogotá. 2014.
15. A. Kerr, "On the Dynamic response of a prestressed beam", *Journal of Sound and Vibration* 49: 569-573, 1976.
16. A. Materazzi, M. Breccolotti, F. Ubertini, I. Venanzi, "Experimental modal analysis for assessing prestress force in PC bridges: a sensitivity study", In 3rd International Operational Modal Analysis Conference: Curran Associates, Inc. (Ed.), Portonovo, Italy, 2009.
17. M. Breccolotti, F. Ubertini, I. Venanzi, "Natural frequencies of prestressed concrete beams: theoretical prediction and numerical validation", In 3rd International Operational Modal Analysis Conference: Curran Associates, Inc. (Ed.), Portonovo, Italy, 2009.
18. American Association of State Highway and Transportation Officials, AASHTO. *Standard Specifications for Highway Bridges*. Washington, D.C AASHTO LRFD Bridge Design Specification, Sixth edition, 2012.
19. Kinometrics Inc. (2016). [On line]. Available: <https://kinometrics.com/>.
20. J. Leis, "Sampled signals and digital processing, digital signal processing using MATLAB for students and researchers", Singapore, John Wiley & Sons Inc., pp 383, 2011.
21. *Structural Vibration Solutions ARTeMIS Extractor, User's Manual*, Denmark.
22. A. Altunışık, O. Karahasan, A. Genç, F. Okur, M. Günaydin, E. Kalkan, S. Adanur, "Modal parameter identification of RC frame under undamaged, damaged, repaired and strengthened conditions", *Measurement* 124: 260-276, 2018.
23. J. Malveiro, D. Ribeiro, C. Sousa, R. Calçada, "Model updating of a dynamic model of a composite steel-concrete railway viaduct based on experimental tests", *Engineering Structures* 164: 40-52, 2018.
24. R. Brincker, P. Andersen, "Ambient response analysis modal analysis for large structures", In Sixth International Congress on Sound and Vibration: F. Jacobsen (Ed.), Copenhagen, Denmark, 1999.
25. I. Gómez, "Caracterización dinámica experimental de puentes de hormigón simplemente apoyados a partir de pruebas de vibración ambiental", Thesis, Industrial University of Santander, Bucaramanga, 2010.
26. S. Gade, N. Møller, H. Herlufsen, H. Brüel, "Frequency domain techniques for operational modal analysis", In 1st international Operational Modal Analysis Conference, Rune Brincker (Ed.), Copenhagen, Denmark, 2005.

27. L. Vargas, "Propuesta de plan de monitoreo del comportamiento dinámico para la salud estructural del nuevo puente Gómez Ortiz", Thesis, Industrial University of Santander, Bucaramanga, 2016.
28. Y. Tian, J. Zhang, Q. Xia, P. Li, "Flexibility identification and deflection prediction of a three-span concrete box girder bridge using impacting test data", *Engineering Structures* 146: 158-169, 2017.
29. P. Moradipour, T. Chan, C. Gallage, "Benchmark studies for bridge health monitoring using an improved modal strain energy method", *Procedia Engineering* 188: 158-169, 2017.
30. C. Rainieri, F. Magalhaes, "Challenging aspects in removing the influence of environmental factors on modal parameter estimates", *Procedia Engineering* 199: 2244-2249, 2017.

### LIST OF FIGURES

Figure 1. a) La Unión viaduct side view, b) La Unión viaduct cross section.

Figure 2. a) Calibration period vs number of elements (north section), b) Calibration period vs number of elements (south section), c) Imposed Loads, Bridge Segments and Pylon (FE Model North Section).

Figure 3. Numerical Mode Shapes (North Section)

Figure 4. Numerical Mode Shapes (Construction Stage 2).

Figure 5. Experimentally Determined Mode Shapes.

Figure 6. Experimental and Numerical Mode Shapes (North Section).

Figure 7. Experimental and Numerical Mode Shapes (South Section).

Figure 8. Experimentally Derived Mode Shapes (Construction Stage 2).

Figure 9. Experimental and Numerical Obtained Mode Shapes (Construction Stage 2).

*Received 07.03.2019 , Revised 04.12.2019*